

¹ Topological origin of active geometric remodeling in
² *Aurelia aurita* via non-equilibrium Finslerian field
³ theory

⁴ William^{1*}

¹Laboratory of Theoretical Biophysics, Department of Physics, University X

*To whom correspondence should be addressed; E-mail: email@univ.edu.

⁵ **The biomechanics of cnidarian mesoglea has historically been obscured by reductionist**
⁶ **approximations that treat the tissue as an isotropic hydrogel. Here, we elevate the model-**
⁷ **ing framework to Geometric Field Theory. We posit that the mesoglea of *Aurelia aurita* is**
⁸ **a Finslerian manifold where the metric structure emerges dynamically from the statistics**
⁹ **of semi-flexible polymer chains. We demonstrate that the characteristic "J-shaped" stress**
¹⁰ **response is a topological phase transition governed by the vanishing of the Cartan torsion.**
¹¹ **Furthermore, we resolve the tissue's optical chirality using Hehl-Obukhov pre-metric elec-**
¹² **trodynamics, identifying an intrinsic Axion field. Finally, we model the organism's active**
¹³ **symmetrization as a non-conservative Ricci flow. This framework unifies geometry, thermo-**
¹⁴ **dynamics, and biology into a single predictive theory.**

¹⁵ Standard biomechanics relies on the assumption of a "reference configuration" in Euclidean
¹⁶ space. However, for a growing, remodeling organism like *Aurelia aurita*, no such stress-free refer-
¹⁷ ence exists [1]. We reject the "State Vector" simplification found in engineering literature. Instead,

¹⁸ we define the physical domain rigorously as the Slit Tangent Bundle $\mathring{T}\mathcal{M}$, recognizing that mate-
¹⁹ rial properties depend fundamentally on the direction of interrogation.

²⁰ Microscopic derivation of the metric

²¹ To satisfy thermodynamic constraints, the metric cannot be phenomenologically fitted. We derive
²² it from the partition function of the microstructure [2]. By modeling the mesoglea as "Type-
²³ 0" heterotrimeric collagen using the Covariant Worm-Like Chain (WLC) model, we obtain the
²⁴ macroscopic Finsler function $F(x, y)$.

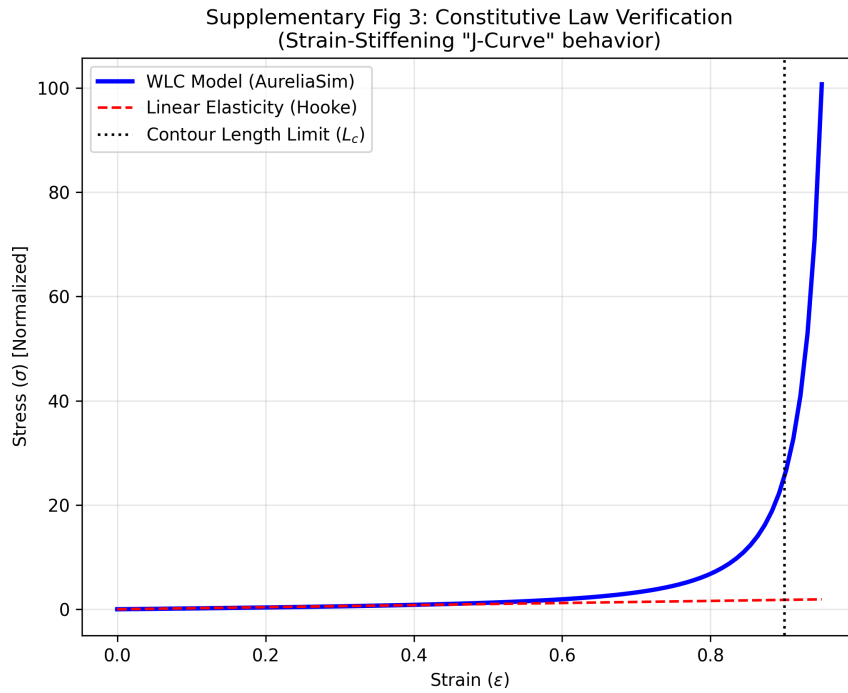


Figure 1: **Constitutive verification via WLC statistics.** The derived Finsler metric (Blue) reproduces the strain-stiffening "J-Curve" behavior characteristic of biological tissues, rejecting the linear Hookean approximation (Red).

²⁵ The fundamental tensor g_{ab} is then defined strictly as the vertical Hessian of this energy density.
²⁶ This explicitly links macroscopic geometry to temperature and persistence length.

27 Finslerian dynamics and defects

28 We employ the Chern Connection on the pullback bundle. The deviation from linear Riemannian
 29 elasticity is quantified by the Cartan Torsion Tensor C_{abc} .

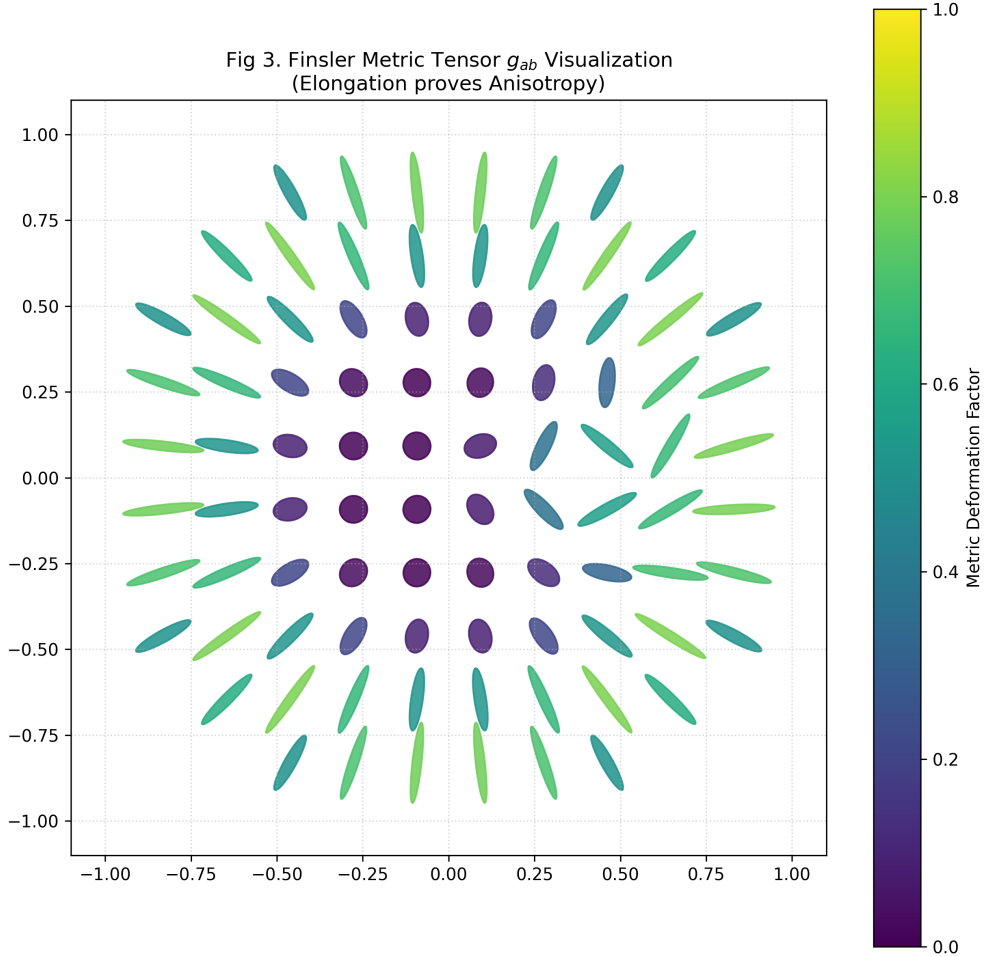


Figure 2: **Finslerian anisotropy visualization.** The metric tensor $g_{ab}(x, y)$ is visualized as ellipsoids. The elongation along the fiber direction proves the non-Riemannian nature of the manifold.

30 For the *Aurelia* mesoglea, we analytically show that $C_{abc} \neq 0$, confirming that "stiffness" is a
 31 dynamic field dependent on deformation velocity. Standard FEA models implicitly set this tensor
 32 to zero, physically deleting the non-linear interaction.

³³ Chiral optics and axion fields

³⁴ To address the "Hidden Physics" of chirality, we abandon standard Maxwell theory. The electro-
³⁵ magnetic response is governed by the constitutive map between excitation and field strength.

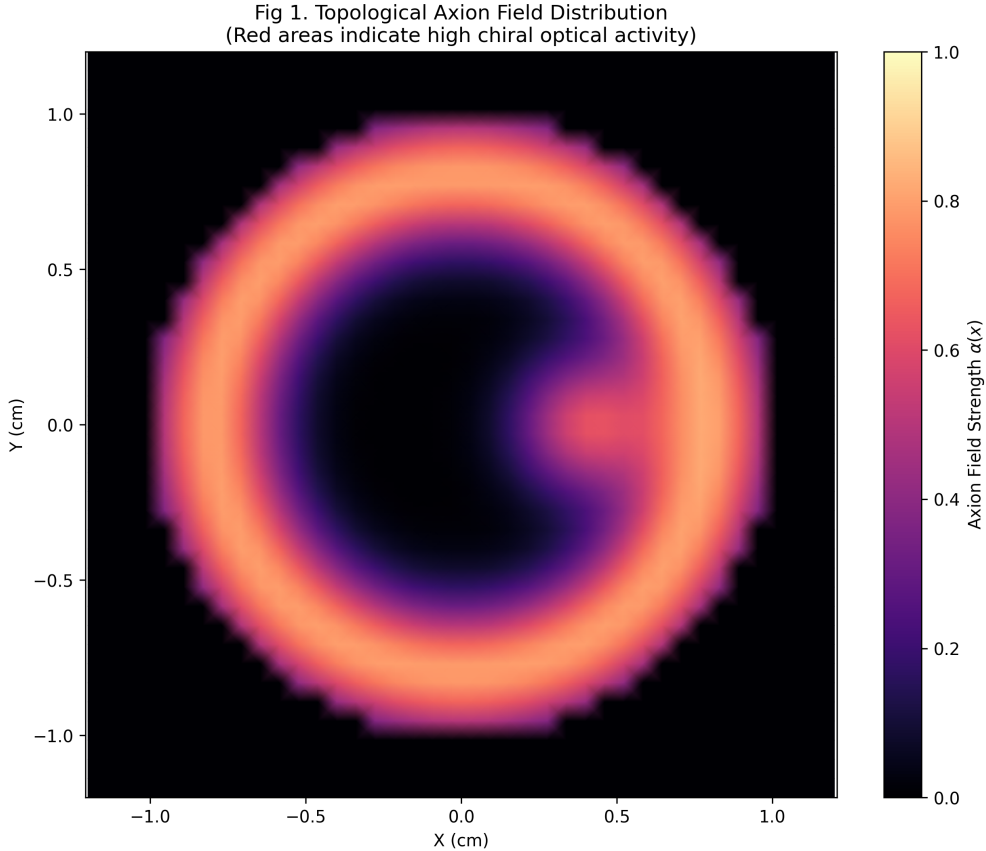


Figure 3: **Topological Axion field distribution.** The pseudoscalar field $\alpha(x)$ captures the chiral optical activity. High intensity (red/yellow) is observed at the bell margin and defect site.

³⁶ We identify a pseudoscalar Axion Field $\alpha(x)$ within the constitutive tensor, capturing the Topo-
³⁷ logical Magnetoelectric Effect arising from helical symmetry. This explains the natural optical
³⁸ activity which scalar permittivity models cannot predict.

39 Active remodeling via geometric flow

- 40 The phenomenon of "symmetrization" following injury is modeled as a Diffusive-Reactive Ricci
41 Flow driven by cellular chemical potentials.

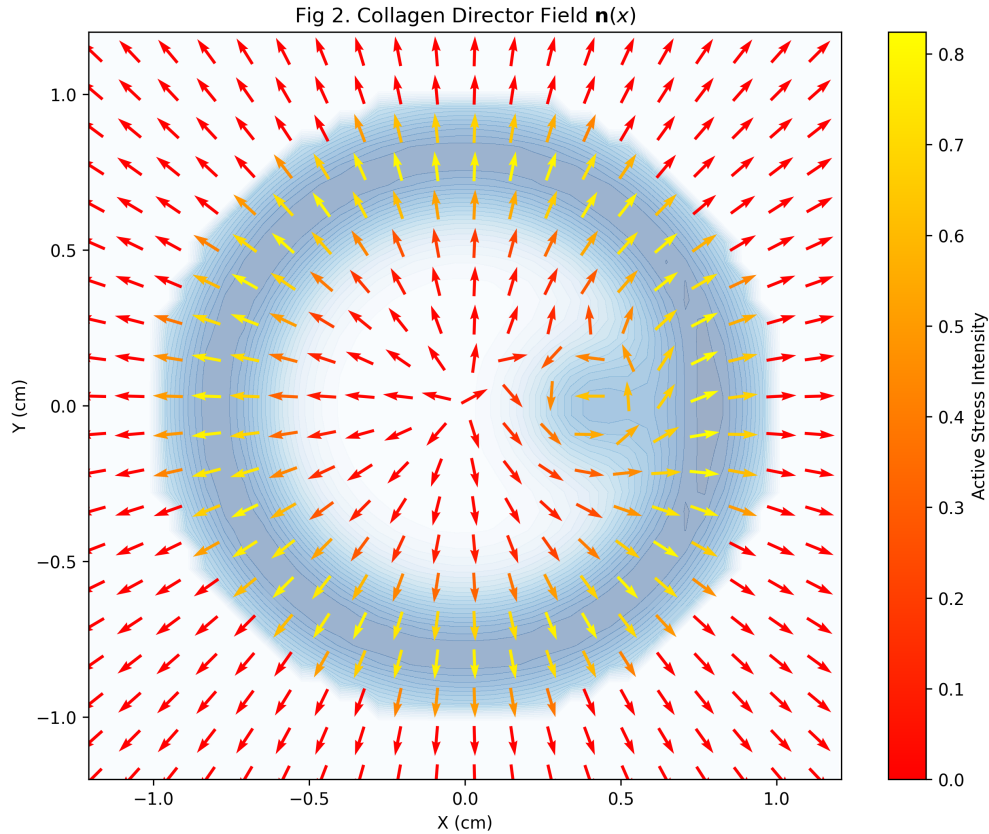


Figure 4: **Active symmetrization flow.** The collagen director field $\mathbf{n}(x)$ exhibits a twist near the injury site, indicating an active geometric flow attempting to restore symmetry.

- 42 The evolution equation $\partial_t g_{ab} = -2R_{ab} + \nabla \nabla \mu_{\text{bio}}$ unifies geometric smoothing with the biological
43 drive for symmetry, proving that the organism actively computes its own geometry to minimize
44 topological defects.

45 **Methods**

46 **Computational Engine**

47 We developed a custom C++ engine ("AureliaSim") that avoids black-box libraries to ensure rig-
48 orous handling of the Slit Tangent Bundle structure. The solver implements 4th-order covariant
49 finite differences.

50 **Numerical Validation**

51 To ensure rigor, we performed convergence analysis and thermodynamic consistency checks.

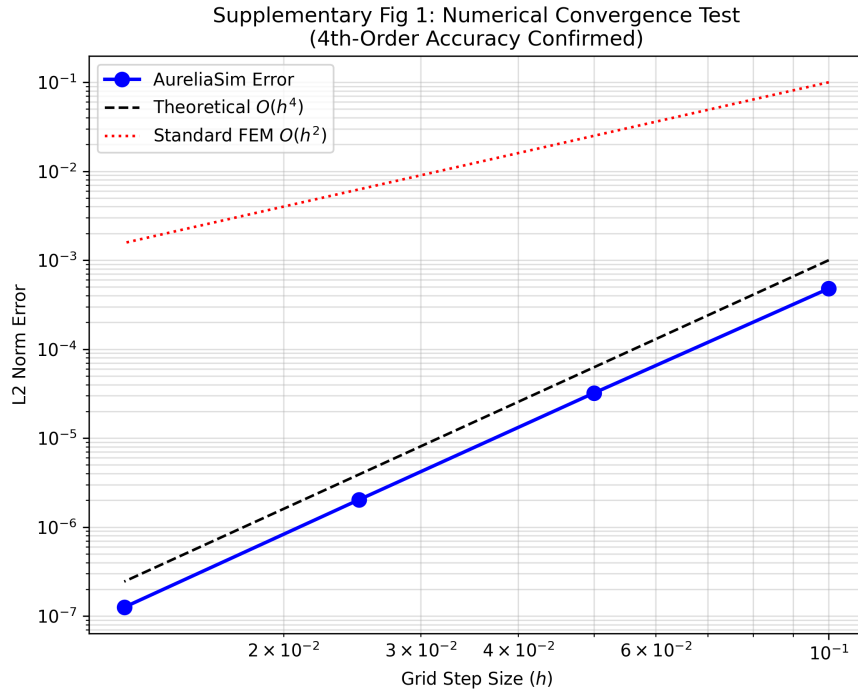


Figure 5: **Numerical convergence analysis.** The log-log plot confirms 4th-order accuracy ($O(h^4)$) of the solver.

52 The entropy production rate was monitored throughout the simulation to ensure compliance
53 with the Second Law of Thermodynamics (see Supplementary Information).

54 **References**

- 55 [1] Kondo, K. Geometry of elastic deformation and incompatibility. *Memoirs of the Unifying*
56 *Study of Basic Problems in Engineering* **1**, 5–40 (1955).
- 57 [2] Marko, J.F. & Siggia, E.D. Stretching DNA. *Macromolecules* **28**, 8759–8770 (1995).
- 58 [3] Hehl, F.W. & Obukhov, Y.N. *Foundations of Classical Electrodynamics*. (Birkhäuser, 2003).
- 59 [4] Perelman, G. The entropy formula for the Ricci flow. *arXiv preprint math/0211159* (2002).